Investigations of Bis-chromophore Systems: Relationship between Spectral Behaviour and Charge Transfer in 2-(3-coumaroyl)-benzopyrylium Perchlorates

E.V. Sanin[a,b], A.I. Novikov [c], A.D. Roshal [a,b]

[a] *Institute of Chemistry, V.N. Karazin Kharkiv National University, Kharkiv, Ukraine*

[b] *SSI "Institute for Single Crystals" of National Academy of Sciences of Ukraine, Kharkiv, Ukraine*

[c] *Guard Department at National Technical University "Kharkiv Polytechnic Institute"*

saninedward@gmail.com

The dependence of spectral properties and interfragmental charge transfer (ICT) on excitation, relaxation and excited state deactivation of 2-(3-coumaroyl)-benzopyrylium perchlorates has been analyzed. It was found that the positions of emission bands and rate constants of radiationless deactivation linearly correlate with ICT upon excited state deactivation, and Stokes' shifts of fluorescence demonstrate linear dependence on ICT upon structural relaxation in the excited state.

Introduction

Bis-chromophore systems are suitable models for photometric investigations of the interfragmental charge transfer and energy transfer, as well as they can be used for the construction of new indicators, photochromes and biological probes [1]. The present work is devoted to investigations of 2-(3-coumaroyl)-benzopyrylium perchlorates (CBP) – bis-chromophore systems including coumarin (*C*) and benzopyrylium (*BP*) fragments (Scheme 1). The majority of dyes containing coumarin chromophore has high quantum yields of fluorescence, that's why they are frequently used as fluorescent markers and indicators [2, 3]. Coumarin derivatives often demonstrate solvatochromic effects [2, 4], which allows to use them as medium polarity sensors. Benzopyrylium derivatives are sensitive to medium nucleophility, demonstrate photochromism and have a pH-dependent fluorescence [5].

Scheme 1. Structures of the investigated CBP.

	R₁	R₂
I	H	N(CH₃)₂
II	N(CH₃)₂	H
III	N(CH₃)₂	N(CH₃)₂
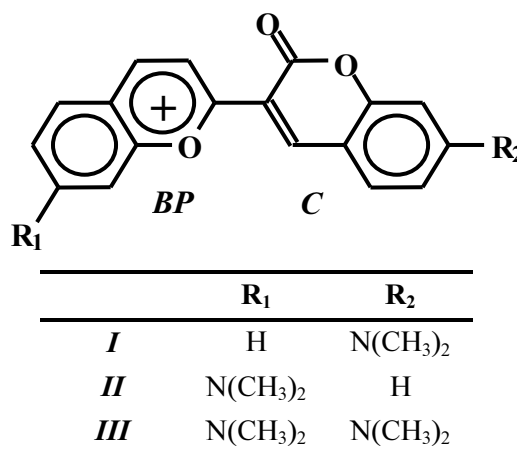
The dihedral angle between *C* and *BP* in the CBP cations is close to zero that ensures maximal coupling of the fragments. The linkage of *C* and *BP* leads to the transfer of negative charge from *C* to *BP* fragment that results in the growth of the positive charge on the coumarin moiety. The electronic structure of the fragments, thus, differs from that of the unconnected benzopyrylium and coumarin chromophores, which explains the unusual spectral behaviour of the CBP cations. The

excitation of CBP changes electron-donating and electron-withdrawing properties of *C* and *BP* that leads to an additional interfragmental charge transfer (ICT).

The present work was aimed to investigate the electronic structure and spectral properties of CBP dimethylamino derivatives with different redistribution of the positive charge between fragments in the ground state and ICT upon excitation.

Results and discussion

Theoretical estimations of charge redistribution between *C* and *BP* in the ground state and upon excitation were carried out using DFT and TD DFT methods. The charge redistribution in the ground state was determined relatively to a model CBP system, where the dihedral angle between *C* and *BP* is 90°, and the charge on *BP* fragment is +1. The value $1 - q_{BP}$ corresponds to the quantity of negative charge going from *C* to *BP* fragment. The interfragmental charge transfer upon excitation was calculated relatively to the charge on the *BP* fragment in the ground state. The obtained results are listed in Table 1.

In the case of non-substituted CBP investigated previously [6], *BP* has charge +0.706ē corresponding to the transfer of 0.294ē from *C* to *BP*, followed by the CBP ion flattening. The introduction of the electron-donating dimethylamino group in *C* increases the electron-donating ability of this fragment, whereas the dimethylamino group connected to *BP* decreases its electron-accepting ability.

In the result, *I* with the dimethylamino group introduced to *C* demonstrates a substantial growth of the interfragmental redistribution of the positive charge (the charge on BP is +0,589 ē), and, when the dimethylamino group is connected to *BP*, the delocalization of the positive charge is minimal, and the charge on *BP* (+0,793ē) is higher than in unsubstituted CBP. *III* with dimethylamino groups in both *C* and *BP* fragments

Table 1. Charges on the benzopyrylium fragment, inter-fragmental charge transfer (ICT) and dipole moments in the ground and excited states obtained by DFT/TD DFT methods*.

	Charges on the benzopyrylium fragment, ($\bar{e}$)				ICT upon excitation, ($\bar{e}$)	ICT upon relaxation in the excited state, ($\bar{e}$)	ICT upon excited state deactivation, ($\bar{e}$)	$\Delta\mu_{S_0 \to S_1^{FC}}$, (D)
	S_0	S_1^{FC}	S_1	S_0^{NR}				
I	0.589	0.487	0.505	0.666	0.102	-0.018	-0.161	0.67
II	0.793	0.797	0.891	0.734	-0.004	-0.094	0.157	1.59
III	0.685	0.637	0.543	0.741	0.048	0.094	-0.198	1.90

*Positive charges are given for the ground state (S_0), Frank-Condon excited state (S_1^{FC}), relaxed excited state (S_1) and non-relaxed excited state (S_{NR}). ICT values correspond to the transfer of the negative charge from coumarin to benzopyrylium fragment. $\Delta\mu_{S_0 \to S_1^{FC}}$ – dipole moment changes upon excitation ($S_0 \to S_1^{FC}$).

shows similar charge redistribution to that for unsubstituted CBP, although the $N(CH_3)_2$ group in *C* demonstrates higher electron-donating ability.

In the Franck-Condon excited state $(S_0 \rightarrow S_1^{FC})$ the influence of dimethylamino groups increases. The data in Table 1 show that the intensity of ICT upon excitation linearly depends on the redistribution of positive charge in the ground state (Figure 1): the higher the charge on the BP fragment, the lower the ICT. In the case of *II* with the maximal positive charge on *BP*, ICT C→BP upon excitation is blocked.
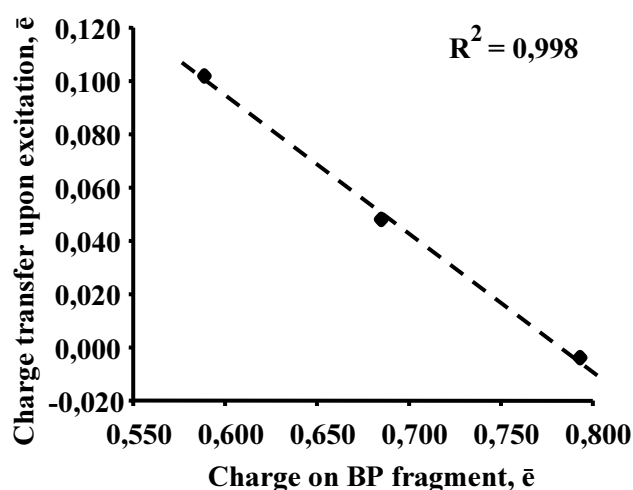

Figure 1. Plot of the $S_0 \rightarrow S_1^{FC}$ charge transfer against the value of positive charge on *BP*.

During the structural relaxation process in the excited state $(S_1^{FC} \rightarrow S_1)$ directions and intensities of ICT are individual for each compound. No dependence of ICT on the charges on fragments in S_0 and S_1^{FC} was found.

ICT upon excited state deactivation $(S_1 \rightarrow S_0^{NR})$ is proportional $(R^2 = 0.981)$ to the sum of charges transferred upon excitation $(S_0 \rightarrow S_1^{FC})$ and excited-state structural relaxation process $(S_1^{FC} \rightarrow S_1)$, but it occurs in the opposite direction. The dependence found can be described by the following equation: $\Delta q(S_1 \rightarrow S_0^{NR}) = -0.636 \times (\Delta q(S_0 \rightarrow S_1^{FC}) + \Delta q(S_1^{FC} \rightarrow S_1))$.

To estimate the relationship between ICT processes upon excitation, relaxation, deactivation of the excited state and spectral behaviour, we have measured spectral parameters of CBP in dichloromethane and acetonitrile (Table 2).

The data presented in Table 2 show that long-wavelength bands in absorption spectra undergo a hypsochromic shift on going from dichloromethane to acetonitrile. Taking into account the growth of CBP dipole moment upon excitation (Table 1) the observed spectral phenomenon cannot be explained by influence of the medium polarity. The most probable cause of hypsochromic shift seems to be the formation of nucleophile complexes between the BP fragment and acetonitrile molecules, which were found earlier in the solutions of 2-phenylbenzopyrylium salts [5, 7]. The strength of a nucleophile complex increases with a growth of positive charge on *BP* fragment. Upon excitation, the charge on *BP* decreases, therefore the stability of the nucleophile complex of CBP (and stabilizing effect of nucleophile solvent) must be lower in the excited state than in the ground one. This results in the increase of the long-wavelength transition energy in the absorption spectra. In the case of *II*, where, according to the calculations, the positive charge delocalization upon excitation does not take place, the minimal hypsochromic shift in absorption spectra has been found.

Table 2. Spectral characteristics of CBP in dichloromethane and acetonitrile.

	Solvent	λ_{abs}, (nm)	ν_{abs}, (cm^{-1})	λ_{fl}, (nm)	ν_{fl}, (cm^{-1})	$\Delta\nu_{St}$, (cm^{-1})	φ	τ, (ns)	$k_f \times 10^{-7}$, (s^{-1})	$k_d \times 10^{-8}$, (s^{-1})
I	CH$_2$Cl$_2$	627	15950	689	14515	1435	0.12	2.8	4.3	3.1
	CH$_3$CN	612	16340	695	14390	1950	0.02	2.2	0.9	4.5
II	CH$_2$Cl$_2$	554	18050	668	14970	3080	0.01	1.1	0.9	9.0
	CH$_3$CN	548	18250	683	14640	3610	0.009	1.5	0.7	6.6
III	CH$_2$Cl$_2$	670	14925	695	14390	535	0.57	3.6	16.0	2.6
	CH$_3$CN	653	15315	700	14285	1030	0.35	2.4	15.0	2.7

* λ_{abs}, λ_{fl} – wavelengths of absorption and emission band maxima, ν_{abs}, ν_{fl} – wave numbers of absorption and fluorescence band maxima, $\Delta\nu_{St}$ – Stokes' shifts of fluorescence, φ, τ – quantum yield and lifetime of fluorescence, k_f and k_d – emission and rate constants of the radiationless deactivation.

On going to acetonitrile, *I* and *III* show bathochromic shifts of emission bands and, simultaneously, a substantial decrease of quantum yields of fluorescence and lifetimes in the excited state. *II* demonstrates a greater bathochromic shift of emission band under the increasing of medium polarity, however it has low fluorescence intensity independent on solvent nature. Stokes' shifts of fluorescence of *II* are 2-3 times greater, than those of *I* and *III*, which indicates more significant structural relaxation of *II* in the excited state.

It is worth to note a linear plot (R^2= 0.982 for dichloromethane and 0.965 for acetonitrile) of the rate constants of the radiationless deactivation (k$_d$) and the positions of emission band maximums in CBP fluorescence spectra. Red shift of the bands results in the increase of k$_d$. This means that the main way of radiationless deactivation is radiationless internal conversion, due to low values of S$_1\rightarrow$S$_0$ transition energy.

Comparison of the positions of absorption bands and calculated values of ICT upon the excitation does not show any correlation. A probable cause of that is the influence of the above mentioned specific interactions of CBP derivatives with solvent molecules, as well as the influence of medium polarizability, which were no taken into account in the calculations.

Meanwhile, ICT upon the excited state deactivation shows good correlation with the positions of emission bands and, correspondingly, with the rate constants of radiationless deactivation (Figure 2). The best correlation was observed for CBP solutions in dichloromethane (R^2 = 0.988), where the influence of environment is minimal. Hence, it is possible to conclude that fluorescent properties of CBP derivatives are directly connected with ICT.

Stokes' shifts of fluorescence reflect relaxation processes in molecules, and that is why the comparison of $\Delta\nu_{St}$ and ICT for the relaxation process S$_1^{FC}\rightarrow$S$_1$ seems to be true. The dependence
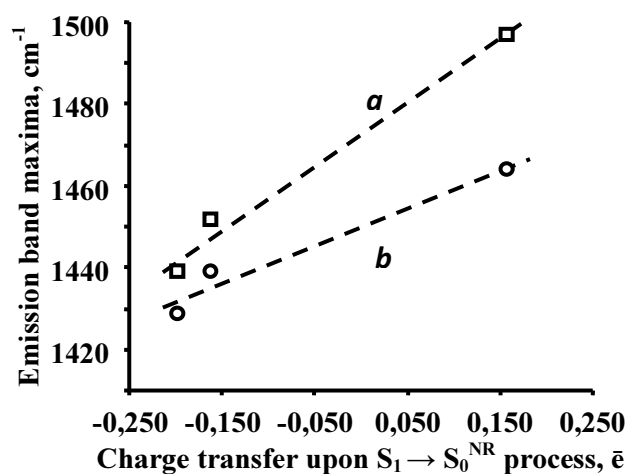
Figure 2. Plot of emission band maxima against $S_1 \rightarrow S_0^{NR}$ ICT (*a* – in dichlorome-thane, *b* – in acetonitrile)

between Δq ICT and Δv_{St} is also linear with high correlation coefficients ($R^2 = 0.926$ for both solvents).

Conclusions

The comparison of the experimental and theoretical data shows that such spectral characteristics of CBP derivatives as positions of emission bands, Stokes' shifts of fluorescence, and rate constants of radiationless deactivation are concerned with the charge transfer between coumarine and benzopyrylium fragments. The obtained dependences allow to make directed synthesis of charged bis-chromophore systems with high sensitivity to medium properties and improved spectral characteristics.

Experimental part

Spectral parameters of the CBP perchlorates were measured in dichloromethane and acetonitrile solutions, CBP concentrations were in the range of $1.0\text{-}5.0 \times 10^{-5}$ M. Absorption spectra were measured on a Hitachi U3210

spectrophotometer, emission spectra and quantum yields of fluorescence were measured on a Varian Cary Eclipse spectrofluorimeter (fluorescence standard – Cy5 in water ($\varphi = 0.25$)), lifetimes were measured on a ISS ChronosFD fluorimeter (fluorescence standard – Alexa 647 in water ($\tau = 1.1$ ns)).

Calculations of Mulliken charges on the CBP fragments were carried out using DFT and TD DFT levels of theory [8] with the B3LYP functional and cc-pVDZ basis set implemented in the Gaussian 09 program package [9].

References

[1] B.M. Krasovitski, L.M. Afanasiadi, Mono- and bis-fluorophores, Ed. of Institute for Monocrystals, Kharkiv, **2002**.

[2] G.S. Shankarling, K.J. Jarag, *Resonance*, **2010**, *N.9*, 804-818

[3] G. Jones, W. R. Jackson, C. Choi, W.R. Bergmark, *J. Phys. Chem.*, **1985**, *89*, 294-300.

[4] R. Dondon, V.P. Khilya, A.D. Roshal, S. Fery-Forgues. *New J. Chem.*, **1999**, *23*, 923-927.

[5] A.D. Roshal, D.Y. Minayev, V.L. Koval, A.I. Novikov, *Opt. Spectrosc.,* **1998**, *85*, 705-710.

[6] E.V. Sanin, A.I. Novikov, A.D. Roshal, *Funct. Mater.*, **2013**, *in press*.

[7] A.D. Roshal, D.Yu.Minayev, Yu.F. Pedash, A.I. Novikov, *Pol. J. Chem.*, **2002**, *76*, 1301-1321.

[8] J.K. Labanowski, in: Density Functional Methods in Chemistry, Springer-Verlag, New York, **1991**.

[9] M.J. Frisch, G.W. Trucks, et al. Gaussian 09, rev. C.02, Wallingford, CT, **2004**.